Published in final edited form as:
Angiogenesis. 2010 June ; 13(2): 75–85. doi:10.1007/s10456-010-9170-4.

Visualizing vascular permeability and lymphatic drainage using labeled serum albumin

Katrien Vandoorne,
Department of Biological Regulation, Weizmann Institute, Rehovot 76100, Israel

Yoseph Addadi, and
Department of Biological Regulation, Weizmann Institute, Rehovot 76100, Israel

Michal Neeman
Department of Biological Regulation, Weizmann Institute, Rehovot 76100, Israel

Michal Neeman: michal.neeman@weizmann.ac.il

Abstract

During the early stages of angiogenesis, following stimulation of endothelial cells by vascular endothelial growth factor (VEGF), the vascular wall is breached, allowing high molecular weight proteins to leak from the vessels to the interstitial space. This hallmark of angiogenesis results in deposition of a provisional matrix, elevation of the interstitial pressure and induction of interstitial convection. Albumin, the major plasma protein appears to be an innocent bystander that is significantly affected by these changes, and thus can be used as a biomarker for vascular permeability associated with angiogenesis. Traditionally, albumin leak in superficial organs was followed by colorimetry or morphometry with the use of albumin binding vital dyes. Over the last years, the introduction of tagged-albumin that can be detected by various imaging methods, such as magnetic resonance imaging and positron emission tomography, opened new possibilities for quantitative three dimension dynamic analysis of permeability in any organ. Using these tools it is now possible to follow not only vascular permeability, but also interstitial convection and lymphatic drain. Active uptake of tagged albumin by caveolae-mediated endocytosis opens the possibility for using labeled albumin for vital staining of cells and cell tracking. This approach was used for monitoring recruitment of perivascular stroma fibroblasts associated with tumor angiogenesis.

Keywords

Vascular permeability; Interstitial convection; Lymphatic drain; Albumin; VEGF; Imaging; Cell tracking

Introduction

Angiogenesis, the sprouting and expansion of the vascular bed, is often triggered by the activity of one central angiogenic growth factor, vascular endothelial growth factor (VEGF), identified not only as a mitogen for endothelial cells, inducing their proliferation [1], but also by its potent ability to induce permeability of blood vessels [2]. Thus, vascular permeability is a common hallmark of normal and pathological angiogenesis and VEGF was also named vascular permeability factor (VPF) [2,3].

Correspondence to: Michal Neeman, michal.neeman@weizmann.ac.il.

Vascular permeability induced by VEGF is not a consequence of perforations in the vessel wall, but rather is due to specific endothelial cell structures, the vesiculo-vacuolar organelles (VVO); which bud at the vessel lumen face and allow transport of blood fluid across the vessel wall. VVO formation is activated by VEGF as well as by histamine [4]. Vascular permeability is interpreted and measured differently by researchers from different research fields [5]. While physiologists considered the vessels as passive barriers with pores of various sizes, through which materials pass by random walk diffusion, vascular biologists regard vascular permeability with respect to the bulk transfer of plasma macromolecules and their accumulation in the tissue.

An important tool that enabled the discovery of VEGF activity on vascular permeability was the *Miles Assay*, in which a vital dye that binds to serum albumin, such as Evans Blue, is administered intravenously. Intradermal administration of the material that induces vascular permeability, leads within minutes to ‘blueing’ of a growing circle surrounding the injection site [6]. The aim of this review is to introduce the significant advances over the last years in utilizing non invasive imaging technologies for visualizing vascular permeability and lymphatic drain using labeled albumin. The review will start with the methodology for determination of blood volume fraction and permeability surface area product by MRI using labeled albumin, followed by the primary methods used for validation of albumin-based analysis of blood volume and vessel permeability using fluorescence microscopy. We will then review the use of these tools for analysis of tumor and non-tumor angiogenesis, followed by review of the use of labeled albumin for MRI analysis of interstitial convection and lymphatic drain. Finally we will describe briefly the use of labeled albumin for in vivo tracking of cell recruitment in angiogenesis.

Albumin is the most abundant plasma protein in the blood stream (35–50 g/l in human), and one of the major protein synthesis products of the liver (approximately 0.7 mg/h for every gram of liver tissue), characterized with an average half-life of 19 days [7]. It consists of a single polypeptide chain of 581 residues and exists in a multi-domain structure with complex ligand binding specificities [8]. The Albumin molecule is highly organized with hydrophobic internal structure, stabilized by disulfide bonds, and a relatively flexible hydrophilic surface [9]. Its structure and abundance defines its binding capabilities and physiological role, it binds long chain fatty acids, bilirubin, heme breakdown products, copper nickel and more. In addition it has a critical role in blood osmotic control [7]. Therapeutically it is of high importance as it binds a variety of compounds, and therefore acts as a drug carrier for various drugs for different targets.

The diverse binding capabilities of albumin enables to link to it external groups such as drugs, fluorescent molecules and radioisotopes, making it a powerful carrier for drugs and contrast probes. Macromolecular contrast media provide an advantage for imaging angiogenesis, as the angiogenic vessel wall is permeable to such contrast media, while resting blood vessels do not allow passive leak of plasma proteins or other macromolecules (Fig. 1). Indeed, GdDTPA labeled albumin (66.6 KD), shows increased specificity in tumor staging and in detection of response to anti-angiogenic therapy [10–12]. The characteristics of albumin makes it highly useful as a contrast agent in tumor angiogenesis, tumor microvessels have pore size of 100 to 1,200 nm in diameter [7,13,14] enabling albumin, with an effective diameter of 7.2 nm, to extravasate into the tumor, but not out of normal vasculature, resulting in a tumor specific accumulation. Being an abundant endogenous plasma protein, albumin can be specifically internalized by some cells, through the caveolae pathway. This specific uptake can be used in order to load contrast material into cells, and for tracking cell migration by non-invasive imaging.

Noninvasive MRI allows three-dimensional (3D) visualization of the complex vascular bed [15] and offers the advantage of unique soft tissue contrast, high penetration depth in tissue and a wide range of experimental protocols with different contrast mechanisms. The microvasculature includes those blood vessels of a diameter of 100 μm and smaller. This upper limit of vessel diameter coincides with the spatial resolution of high-resolution small animal MR scanners. Therefore, dynamic contrast enhanced (DCE) MR imaging of microvasculature, where physiological information from vessels that are not directly visible in the images is extracted, differs from MR angiography, where only large blood vessels are imaged [16].

Albumin can be covalently linked to 25–35 (Gd-DTPA) groups, in order to allow its detection by MRI through the increase in the rate of the longitudinal R_1 relaxation of water, resulting in signal enhancement. After intravenous administration, it shows slow clearance from the circulation, and its volume of distribution corresponds closely to the body's relative blood volume, thus serving as a blood pool agent [13,17]. Due to the lower tumbling rate of the albumin bound GdDTPA, the r_1- and r_2- relaxivity of this contrast agent, reflecting the efficacy in generating MRI contrast, is substantially higher compared to low-molecular weight contrast agents [10]. This increase in relaxivity raises the sensitivity for its detection by MRI. Addition of biotin can be used for detection of the contrast media in histological sections [18]. In addition, the biotin can be used for altering the pharmacokinetics of the contrast material in circulation through in vivo avidin chase, namely for inducing rapid elimination of the contrast media from circulation by phagocytic macrophages upon intravenous administration of avidin [16]. In addition, albumin can be further modified so as to include fluorescent or NIR tags (Fig. 2a) or additional targeting moieties [16,19] widening the possible in vitro and in vivo follow up methods.

An alternative approach includes low molecular weight contrast media with high affinity to albumin, which can be used for measuring vascular permeability, in a manner analogous to the use of Evans Blue in the Miles Assay. Such a compound, MS-325 was applied in preclinical models as well as for human imaging [20–22].

Determination of blood volume fraction and permeability surface area product

The relatively slow permeability, long half-life in circulation and the relative inertness of albumin-based contrast agents, allow quantification of blood volume fraction (fBV), and permeability (permeability surface area product; PS; Fig. 2b, d). Molecular exchange across the microvascular wall is a fundamental constituent of the function of the microvasculature in perfusing the target tissue. Low molecular weight contrast agent, such as GdDTPA, extravasates in the presence of non-specific channels or pores in the vessel wall. These low molecular weight contrast agents provide a sensitive measure of vascular leak in tissues with inherently very low permeability, such as the central nervous system, where the blood brain barrier prevents extravasation of small molecules. However in other tissues, in which the low-molecular-weight materials easily extravasate, the initial distribution volume of these contrast agents after intravenous bolus injection, approximate the extracellular space, comprising both vascular and interstitial space. As fractional blood volume and vascular permeability with low molecular weight contrast agents are overestimated, it was argued that it would be difficult to accurately measure angiogenesis using such contrast media [12, 23]. In such tissues, high molecular weight contrast agents may provide increased specificity for detection of blood volume fraction and elevation in vascular permeability [24, 25].

Large serum proteins, such as albumin, extravasate through the large fenestrations and VVOs and can accumulate in the extravascular space selectively in regions with elevated vascular permeability [24]. After intravenous bolus injection, the initial distribution volume

of this high-molecular-weight contrast agent approximates the blood volume of the tissue of interest [12].

To correct for variability in contrast media dosage, the tissue concentrations can be normalized by the blood concentration of the contrast agent, measured in a large vein, typically the vena cava, or the right ventricle. For macromolecular contrast agent, the blood volume fraction (fBV), is a measure of (micro)vascular density and is calculated from the ratio between the extrapolated concentration of BSA-GdDTPA at time of administration and the concentration in the blood. The permeability surface area product (PS; min^{-1}), the initial rate of contrast accumulation normalized to the blood concentration. PS reflects the leak of macromolecules out of the blood vessels and their accumulation in the tissues (Fig. 2b, d) [26].

Quantitative determination of the concentration of the contrast material is particularly complicated for MRI due to the indirect detection. The contrast material is revealed through its effect in enhancing the longitudinal relaxation rate R_1 of water. The first step for quantification is the determination of the specific relaxivity r_1 (in $mM^{-1}\ s^{-1}$). The relaxivity depends on the interaction of the contrast material with water and is enhanced by reducing the tumbling rate (e.g by binding to albumin), but is significantly reduced by endosomal uptake, leading to significant 'quenching' of the contrast enhancement, making it MRI invisible. Next, R_1 relaxation rate should be determined before and after administration of the contrast media. The concentration [C] of MRI visible contrast media can then be derived from the linear relation (Eq. 1):

$$R_{1,post}=R_{1,pre}+r_1[C] \quad (1)$$

Validation of the actual distribution of the contrast media in the various tissues (including also MRI invisible endosomal contrast media) can be done by analysis of Gd content using inductively coupled plasma mass spectroscopy (ICP-MS).

Validation of albumin-based analysis of blood volume and vessel permeability by fluorescence microscopy

An inherent requirement for in vivo imaging studies is to provide independent validation for the findings. The 3D advantage of MRI is demonstrated in studies of cross validation between histological and MR rendering of blood vessels [27,28]. The presence and distribution of macromolecular contrast agent can be validated using histological staining for the MRI contrast media through addition of a biotin group generating a dual histology/MR probe biotin-albumin-GdDTPA [29]. The distribution of this contrast media can be detected in histological sections by using an avidin–biotin-complex (ABC) stain, such as avidin-fluorescein isothiocyanate (FITC) [30]. Biotin-albumin-GdDTPA can additionally be directly labeled with fluorescent markers (for example fluorescein (FAM) or rhodamine (ROX) derivatives). Such multiple labels were useful for histological analysis of the extravasation and fate of contrast agent in hyperpermeable microvasculature [30].

As an additional intra-vascular marker, albumin labeled with a fluorescent marker, can be administered intravenously, 3 min before sacrificing the animal. In the short period during which the contrast material is distributed throughout the body, extravasation from blood vessels is negligible, even in areas with leaky blood vessels. Thus this marker provides an independent histological measure of the volume fraction of functional blood vessels, equivalent to MRI data acquired during the early time points after administration of biotin-albumin-GdDTPA. Analysis of this initial enhancement yields the (micro)vascular density (fBV).

Staining of biotinylated MR contrast agent with avidin-FITC or fluorescence microscopy of MR contrast agent labeled with fluorescent markers, yields a histological equivalent representation of the permeability surface area product (PS), corresponding to the leak of macromolecules from the blood vessels and their accumulation in the tissues. These fluorescent markers can be visualized with fluorescent microscopy on histological slices following tissue fixation with Carnoy's solution. Caution should be used in organs with high endogenous levels of biotin.

Notably, a mismatch between the distribution of the contrast material as detected by ICP-MS and by histology from that detected by MRI, can arise from quenching of relaxivity by endosomal uptake of the contrast material [16].

Imaging tumor angiogenesis using (biotin)-BSA-GdDTPA

Angiogenesis is necessary for tumor growth and metastasis [31]. MRI monitoring of tumor angiogenesis has been extensively investigated in the last decades. DCE-MRI, using albumin-labeled contrast agent, allows in vivo quantification of angiogenesis rendering both measures of microvascular density (fBV) and permeability (PS; see above).

The switch to an angiogenic phenotype is a fundamental determinant of neoplastic growth and tumor progression [31]. Amplification of the transcription factor hypoxia inducible factor (HIF)-1alpha dependent responses to hypoxia via loss of p53 function, contributes to the angiogenic switch during tumorigenesis. This angiogenic switch was shown by MRI, using albumin-GdDTPA as a macromolecular contrast agent [32]. By deletion of the p53 tumor suppressor gene, promoting the neovascularization and growth of tumor xenografts in nude mice, increased angiogenesis was manifested by elevated vascular volume and vessel permeability [32]. Recently, macromolecular DCE-MRI was applied for mapping vessel density and permeability in islet1, RIP-Tag2 pancreatic tumors [33].

Elevation of capillary permeability, in response to VEGF, leading to extravasation of serum proteins can be detected by MRI using albumin-GdDTPA [11,24,26,30,34]. Macromolecular albumin-based contrast agent was extensively used for early detection of tumor response to antiangiogenic therapy [11,35–38]. MRI using intravascular albumin-GdDTPA could detect the effects of the antiangiogenic agent TNP-470 on the vascular volume and permeability in a prostate cancer model [38]. Reduced activation of both platelet-derived growth factor receptor (PDGFR)-beta and VEGF receptor 2 (VEGFR2) in imatinib-treated mice was demonstrated by macromolecular DCE-MRI [36]. Macromolecular DCE-MRI showed an early measurable predictive biomarker of tumor angiogenesis treatment response. Acute change in vascular leakiness was measurable after a single dose of bevacizumab [35].

The spatial distribution of vascular permeability and vascular maturation could be correlated by sequential analysis of the tumors, using blood oxygenation level dependent (BOLD)-contrast MRI for analysis of vasoreactivity in response to elevated concentration of CO2 (5%; hypercapnia) as a biomarker of vascular maturation, followed by DCE-MRI using biotin-BSA-GdDTPA [39]. A wide range of vascular phenotypes detected were consistent with the expression of VEGF by the tumor cells and expression of growth factors that affect vascular maturation, such as angiopoietin 1 and 2 by the tumor stroma [39] (Fig. 3c).

In an elegant set of studies DCE-MRI using albumin-GdDTPA was also correlated with spectroscopic MR imaging, fluorescence imaging and three dimensional histological reconstruction with an effort to explain the metastatic phenotype [38,40,41]. Vascular volume and permeability were correlated with the extracellular pH in metastatic (MDA-MB-231) and non-metastatic (MCF-7) human breast cancer xenografts [40]. A similar approach was applied also for the study of human prostate cancer xenograft implanted

orthotopically in the prostate or subcutaneously in mice. Hypoxic tumor cells were visualized using an enhanced green fluorescence protein whose expression was regulated by the hypoxia response element. The more metastatic orthotopic tumors, showed higher vascular volume and vascular permeability, which spatially correlated with higher total choline and lower extracellular pH [41].

Following the success of macromolecular DCE-MRI in pre-clinical studies in animal tumor models, applying this technique in human studies and clinics could be of interest for detection of early responses to tumor treatment and characterizing tumor vasculature in cancer patients. Although potential diagnostic applications have been investigated with human serum albumin (HSA-Gd-DTPA), as a prototype macromolecular contrast medium, it is considered a poor candidate for development as a clinical drug, since its elimination is slow and incomplete [17] and protein-based drugs have a potential to induce immunologic toxicity [42]. Thus, alternative macromolecular contrast agents are being tested [43,44]. New polydisulfidebased biodegradable macromolecular contrast agents were compared, with albumin labeled Gd-DTPA in tumor bearing nude mice prostate xenografts, and found promising for characterizing vascularity and angiogenesis with DCE-MRI [45].

An alternative approach is to apply low molecular weight contrast media that bind albumin in the circulation such as MS-325 [22].

Visualizing non-tumor angiogenesis

As originally demonstrated by Senger et al. using the Miles Assay, acute rise of vascular permeability can be induced locally by intradermal administration of VEGF165 [46,47]. Similarly, local extravasation of intravenously administered macromolecular biotin-BSA-GdDTPA was detected by MRI 30 min after intra-dermal administration of VEGF [26]. The accumulation of contrast material in the interstitial space followed mono-exponential saturation kinetics. Delayed administration of the contrast media resulted in reduced leak, demonstrating that the saturation kinetics is not due to equilibration between plasma and the interstitial space, but rather is due to suppression of VEGF-induced vascular permeability. Permeability could be restored by a second bolus of VEGF, showing that the saturation kinetics is primarily due to pharmacodynamics and inactivation of the administered growth factor [26].

Calibrated VEGF levels are crucial not only for pathological tumor angiogenesis, but also for embryonic angiogenesis, the ovarian cycle, endochondral bone formation, wound healing and graft angiogenesis [48]. Uterine receptivity and embryo implantation depend on local induction of angiogenesis and vascular permeability. DCE-MRI and fluorescence microscopy using biotin-BSA-GdDTPA allowed detection and quantitative assessment of mouse embryo implantation sites as early as embryonic day 4.5 (E4.5), and subsequent vascular expansion at E5.5. Vessel permeability was significantly elevated in E4.5 implantation sites relative to non-implanted uterus, showing that elevation of vascular permeability is a very early response preceding E4.5. This functional imaging of implantation by MRI quantifies angiogenesis during normal mouse implantation and allows future evaluation of the involvement of the vasculature in mouse models of impaired implantation (Fig. 2c) [49].

Using this approach, the critical role of dendritic cells in fetal implantation was discovered [50]. Specific ablation of dendritic cells resulted in failure of the critical window of vascular maturation during angiogenesis of the decidua at the fetal implantation site. Thus in the absence of these cells, vascular blood volume fraction was reduced while vessel permeability was significantly enhanced [50].

During endochondral bone formation, blood vessels invade, and supply minerals for long bone formation. Recently, macromolecular DCE-MRI proved to provide high sensitivity for in vivo detection of angiogenesis, at the site of long bone and was able to identify subtle gene dose effects for PKBalpha/Akt1 leading to impaired bone vascularity concomitant with deficiencies in trabecular bone. This indicates that macromolecular DCE-MRI could be used as an early indicator of impaired vascular function in diseases where altered angiogenesis causes impaired skeletal growth (Fig. 2b) [51].

Hyperpermeability, associated with the angiogenic response after ischemic injury induced by ligation of the femoral artery at the right posterior limb in mice, was followed noninvasively by MRI using daily iv administration of biotin-BSA-GdDTPA. MRI provided valuable information on the transient hyperpermeability induced during the early stages of angiogenesis, and its subsequent resolution along with functional recovery from acute hind limb ischemia in mice [52].

Imaging interstitial convection and lymphatic drain

One of the hallmarks of angiogenesis and one of the earliest vascular responses to VEGF is the rapid rise in vascular permeability, leading to extravasation of plasma macromolecules to the interstitial space. Thus, while the chronic exposure to VEGF leads to formation and stabilization of new capillaries, the immediate early response to VEGF includes vasodilation and vascular fenestration. Using albumin labeled with GdDTPA as well as with fluorescence markers made it possible to detect not only the elevated permeability of blood vessels at the site of VEGF administration, but also to reveal how the extravasated albumin is efficiently cleared by interstitial convection and lymphatic drain [26].

Clinical studies linked elevated expression of VEGF with increased lymph node metastases. This association raised the hypothesis that VEGF-induced vascular permeability can augment peritumor interstitial convection and lymphatic drain. Tumors with tetracycline-regulated overexpression of VEGF were used to demonstrate by MRI elevated vascular permeability to biotin-albumin-GdDTPA, followed by interstitial convection, and subsequent lymphatic drain of the contrast media toward the draining lymph node [30] (Fig. 4a).

Although delayed enhancement patterns can be used to follow the direction of convection and drain, they do not provide quantitative kinetic information on the rate of clearance of the extravasated contrast media. In order to measure the rate of clearance, we utilized an in vivo avidin-chase approach, in which slow intravenous administration of avidin induced immediate uptake of the biotinylated albumin-GdDTPA by phagocytic macrophages, leading to complete clearance of the intravascular biotinylated contrast material to the liver and spleen [16] (Fig. 4b). Interestingly, uptake of the avidin bound contrast media by macrophages led to complete elimination of MR contrast, due to sequestration of the complex in intracellular endosomes.

This approach allowed us to separate experimentally between vascular leak and lymphatic drain. Suppression of the over-expression of VEGF abolished vascular permeability and lymphatic drain, providing a direct link between VEGF and peritumor lymphatic function [30]. Convective flux of the contrast material could further be analyzed to ‘draining’ and ‘pooling’ regions through the change in the early and late rate of contrast material accumulation in the tissue [53]. A similar approach was applied for analysis of lymphangiogenesis in bladder cancer [54].

Biotin-BSA-GdDTPA-FAM/ROX was further applied for monitoring changes in blood volume, vascular permeability, interstitial convection, and the early stages of metastatic

dissemination in tumors over-expressing heparanase, an enzyme implicated in tumor invasion, angiogenesis and metastasis [55]. Inter-voxel fluxes of the contrast media yielded maps of interstitial flow direction, showing radial outflow from the tumor, along with directional flow toward the draining lymph node. Changes in MR contrast enhancement in the lymph node preceded the formation of pathologically detectable metastases, suggesting the use of BSA-GdDTPA for detecting the initial stages of lymph node infiltration by metastatic cells [55].

Transplantation of ovarian fragments after cryopreservation, provides a possible promise for overcoming premature ovarian failure in young cancer patients treated by chemo- or radiotherapy. Ovarian graft reception and maintenance was monitored and graft angiogenesis in two transplantation sites was quantified in immunodeficient mice by macromolecular DCE-MRI using biotin-BSA-GdDTPA [56]. Loss of oocytes in ovarian grafts was attributed to impaired perfusion. In an effort to improve graft reception, hormonal and microenvironmental factors were assessed [56,57]. Ovary fragments from young rats were transplanted intramuscularly and subcutaneously in immunocompromised CD1-nude mice. Ovariectomy of the graft recipient prior to transplantation improved follicular development in the grafts along with improved vascular development and increased vascular permeability. Biotin-BSA-GdDTPA, extravasated from the graft neovasculature, showed elevated interstitial convection, draining toward the proximal lymph node, similarly to the pattern of clearance of albumin extravasated from blood vessels in VEGF over-expressing tumors [57] (Fig. 4d).

The use of BSA-GdDTPA for in vivo cell tracking in angiogenesis

The ability to perform cell tracking is critical in many different fields of research, and cell based therapeutics. It can be applied as a monitoring method when cells are implanted in a specific location, and external noninvasive detection is needed [58], or in a wider application when following cell recruitment. The process of cell recruitment occurs in the living organism as part of normal function of a number of systems. Cells can be recruited from a certain reservoir, such as the bone marrow, to act on a remote specific tissue. The process of cellular recruitment accompanies many biological processes including angiogenesis, cancer progression, development, and immune response. Imaging is the only possible methodology for following the dynamics of cell recruitment.

Specifically during angiogenesis multiple cell types are recruited from different locations to assist and participate in construction of the new vessels. Some of these cells affect vessel permeability and thus also lymphatic drain. Performing cell tracking in vivo requires labeling of the cell population of interest, in order to detect its location and route of migration. Labeling of the cells can be done ex vivo followed by injection of the labeled cells, or by targeting the labeling molecule to specific cells. Cell labeling can be achieved using dyes, reporter genes, radiolabeling, Gd based contrast media or iron particles [59–62].

MRI is one of the key methods applied for cell tracking, as it enables whole body imaging with unlimited tissue penetration [63]. Most MRI cells tracking studies use superparamagnetic iron oxide particles. This method of cellular labeling introduces a large magnetic susceptibility which results in easily detectable signal void [61,64]. Another possibility is to label cells by uploading of gadolinium based contrast media, including GdDTPA. In contrast to Gd-DTPA which is rapidly cleared from dying cells, iron particles can be picked up by immune cells producing false secondary labeling [65].

The cellular penetration of conventional low molecular weight gadolinium chelates such as DTPA is generally very low. In order to achieve efficient labeling, modification should be made to the contrast agent or to the cell membrane [66]. Linking Gd-DTPA to BSA changes

the dynamics of the contrast material and its characteristics, enabling high uptake and retention by cells [62]. Fibroblast cells incubated ex-vivo with 10 mg/ml of the Biotin-BSA-Gd-DTPA for 48H, show high cellular labeling, and enhancement in R1 relaxation, with no effect on cell viability. Biotin-BSA-Gd-DTPA labeled fibroblasts administered intraperitonealy showed by MRI a significant recruitment to a remote subcutaneous ovarian carcinoma tumor [61] (Fig. 5b).

The main known route for BSA uptake into the cell is the caveolae pathway, known to be functional in a wide variety of cell types, but most abundant in endothelial cells. As a result of albumin binding to the gp60 protein (albumin binding protein), caveolin-1 and -2 proteins oligomerize, enabling the formation of membrane invaginations in diameter of 60–80 nm. These invaginations perform the endocytosis and transcytosis of albumin across the cell membrane in a single cell level, or the vascular endothelium in the animal level [38,67,68]. Upon internalization of albumin-GdDTPA, relaxivity is attenuated due to endosomal uptake but is subsequently re-gained after re-distribution of the contrast material within the labeled cells [62].

When administered intravenously to mice with subcutaneous ovarian carcinoma tumors, biotin-BSA-GdDTPA remains localized to the vascular and perivascular stroma, and is taken up by perivascular myofibroblasts, however the contrast material remains excluded from the tumor nodules [39,61]. Further modification of the contrast media such as generation of bifunctional daidzein-BSA-GdDTPA, led to enhanced delivery and retention by the tumor cells, across the perivascular stroma myofibroblasts [19].

Summary

In summary, albumin provides a useful carrier for contrast media, and can be used for quantitative determination and mapping of temporal changes in blood volume and vascular permeability during angiogenesis. These parameters can be further correlated spatially and temporally with measurements of additional parameters. In particular, tracing the clearance pathway for albumin extravasating from leaky blood vessels in sites of angiogenesis, provides measures of interstitial convection and lymphatic drain. Lastly, tagged albumin provides a powerful tool for cell tracking. As a naturally occurring protein, it is non toxic and shows specific caveolae mediated cellular uptake. Low molecular weight contrast media with affinity to albumin offers possibility for clinical translation for improved imaging of vascular permeability associated with angiogenesis.

Acknowledgments

This work was supported by the USA NIH R01 CA75334, the DKFZ-MOST cooperational program, the Israel Science Foundation 93/07, The European Commission FP6 Integrated Project MEDITRANS, The European Commission FP7 Integrated Project ENCITE and European Research Council Advanced grant 232640-IMAGO (to MN), and by the Gurwin Foundation. Michal Neeman is incumbent of the Helen and Morris Mauerberger Chair.

References

1. Leung DW, Cachianes G, Kuang WJ, et al. Vascular endothelial growth factor is a secreted angiogenic mitogen. Science 1989;246:1306–1309. [PubMed: 2479986]
2. Dvorak HF. Discovery of vascular permeability factor (VPF). Exp Cell Res 2006;312:522–526. [PubMed: 16430882]
3. Dvorak HF, Nagy JA, Feng D, et al. Vascular permeability factor/vascular endothelial growth factor and the significance of microvascular hyperpermeability in angiogenesis. Curr Top Microbiol Immunol 1999;237:97–132. [PubMed: 9893348]

4. Dvorak AM, Feng D. The vesiculo-vacuolar organelle (VVO). A new endothelial cell permeability organelle. J Histochem Cytochem 2001;49:419–432. [PubMed: 11259444]
5. Nagy JA, Benjamin L, Zeng H, et al. Vascular permeability, vascular hyperpermeability and angiogenesis. Angiogenesis 2008;11:109–119. [PubMed: 18293091]
6. Miles AA, Miles EM. Vascular reactions to histamine, histamine-liberator and leukotaxine in the skin of guinea-pigs. J Physiol 1952;118:228–257. [PubMed: 13000707]
7. Kratz F. Albumin as a drug carrier: design of prodrugs, drug conjugates and nanoparticles. J Control Release 2008;132:171–183. [PubMed: 18582981]
8. Hsia JC, Wong LT, Tan CT, et al. Bovine serum albumin: characterization of a fatty acid binding site on the N-terminal peptic fragment using a new spin-label. Biochemistry 1984;23:5930–5932. [PubMed: 6098304]
9. Doweiko JP, Nompleggi DJ. Role of albumin in human physiology and pathophysiology. JPEN J Parenter Enteral Nutr 1991;15:207–211. [PubMed: 2051560]
10. Schmiedl U, Ogan MD, Moseley ME, et al. Comparison of the contrast-enhancing properties of albumin-(Gd-DTPA) and Gd-DTPA at 2.0 T: and experimental study in rats. AJR Am J Roentgenol 1986;147:1263–1270. [PubMed: 3535459]
11. Pham CD, Roberts TP, van Bruggen N, et al. Magnetic resonance imaging detects suppression of tumor vascular permeability after administration of antibody to vascular endothelial growth factor. Cancer Invest 1998;16:225–230. [PubMed: 9589031]
12. Daldrup H, Shames DM, Wendland M, et al. Correlation of dynamic contrast-enhanced magnetic resonance imaging with histologic tumor grade: comparison of macromolecular and small-molecular contrast media. Pediatr Radiol 1998;28:67–78. [PubMed: 9472047]
13. Ogan MD, Schmiedl U, Moseley ME, et al. Albumin labeled with Gd-DTPA. An intravascular contrast-enhancing agent for magnetic resonance blood pool imaging: preparation and characterization. Invest Radiol 1987;22:665–671. [PubMed: 3667174]
14. Yuan F, Dellian M, Fukumura D, et al. Vascular permeability in a human tumor xenograft: molecular size dependence and cutoff size. Cancer Res 1995;55:3752–3756. [PubMed: 7641188]
15. Neeman M, Provenzale JM, Dewhirst MW. Magnetic resonance imaging applications in the evaluation of tumor angiogenesis. Semin Radiat Oncol 2001;11:70–82. [PubMed: 11146044]
16. Dafni H, Gilead A, Nevo N, et al. Modulation of the pharmacokinetics of macromolecular contrast material by avidin chase: MRI, optical, and inductively coupled plasma mass spectrometry tracking of triply labeled albumin. Magn Reson Med 2003;50:904–914. [PubMed: 14587000]
17. Schmiedl U, Brasch RC, Ogan MD, et al. Albumin labeled with Gd-DTPA. An intravascular contrast-enhancing agent for magnetic resonance blood pool and perfusion imaging. Acta Radiol Suppl 1990;374:99–102. [PubMed: 1966977]
18. van Dijke CF, Mann JS, Rosenau W, et al. Comparison of MR contrast-enhancing properties of albumin-(biotin)10-(gado-pentetate) 25, a macromolecular MR blood pool contrast agent, and its microscopic distribution. Acad Radiol 2002;9(Suppl 1):S257–S260. [PubMed: 12019884]
19. Migalovich HS, Kalchenko V, Nevo N, et al. Harnessing competing endocytic pathways for overcoming the tumor-blood barrier: magnetic resonance imaging and near-infrared imaging of bifunctional contrast media. Cancer Res 2009;69:5610–5617. [PubMed: 19509228]
20. Lauffer RB, Parmelee DJ, Dunham SU, et al. MS-325: albumin-targeted contrast agent for MR angiography. Radiology 1998;207:529–538. [PubMed: 9577506]
21. Caravan P, Cloutier NJ, Greenfield MT, et al. The interaction of MS-325 with human serum albumin and its effect on proton relaxation rates. J Am Chem Soc 2002;124:3152–3162. [PubMed: 11902904]
22. Shamsi K, Yucel EK, Chamberlin P. A summary of safety of gadofosveset (MS-325) at 0.03 mmol/kg body weight dose: Phase II and Phase III clinical trials data. Invest Radiol 2006;41:822–830. [PubMed: 17035873]
23. Brasch RC. New directions in the development of MR imaging contrast media. Radiology 1992;183:1–11. [PubMed: 1549653]
24. Brasch RC, Li KC, Husband JE, et al. In vivo monitoring of tumor angiogenesis with MR imaging. Acad Radiol 2000;7:812–823. [PubMed: 11048879]

25. Bhujwalla ZM, Artemov D, Glockner J. Tumor angiogenesis, vascularization, and contrast-enhanced magnetic resonance imaging. Top Magn Reson Imaging 1999;10:92–103. [PubMed: 10551624]
26. Dafni H, Landsman L, Schechter B, et al. MRI and fluorescence microscopy of the acute vascular response to VEGF165: vasodilation, hyper-permeability and lymphatic uptake, followed by rapid inactivation of the growth factor. NMR Biomed 2002;15:120–131. [PubMed: 11870908]
27. Brey EM, King TW, Johnston C, et al. A technique for quantitative three-dimensional analysis of microvascular structure. Microvasc Res 2002;63:279–294. [PubMed: 11969305]
28. Samoszuk M, Leonor L, Espinoza F, et al. Measuring microvascular density in tumors by digital dissection. Anal Quant Cytol Histol 2002;24:15–22. [PubMed: 11865945]
29. Saeed M, van Dijke CF, Mann JS, et al. Histologic confirmation of microvascular hyperpermeability to macromolecular MR contrast medium in reperfused myocardial infarction. J Magn Reson Imaging 1998;8:561–567. [PubMed: 9626869]
30. Dafni H, Israely T, Bhujwalla ZM, et al. Overexpression of vascular endothelial growth factor 165 drives peritumor interstitial convection and induces lymphatic drain: magnetic resonance imaging, confocal microscopy, and histological tracking of triple-labeled albumin. Cancer Res 2002;62:6731–6739. [PubMed: 12438274]
31. Folkman J. The role of angiogenesis in tumor growth. Semin Cancer Biol 1992;3:65–71. [PubMed: 1378311]
32. Ravi R, Mookerjee B, Bhujwalla ZM, et al. Regulation of tumor angiogenesis by p53-induced degradation of hypoxia-inducible factor 1alpha. Genes Dev 2000;14:34–44. [PubMed: 10640274]
33. Sennino B, Raatschen HJ, Wendland MF, et al. Correlative dynamic contrast MRI and microscopic assessments of tumor vascularity in RIP-Tag2 transgenic mice. Magn Reson Med 2009;62:616–625. [PubMed: 19526501]
34. Ali MM, Janic B, Babajani-Feremi A, et al. Changes in vascular permeability and expression of different angiogenic factors following anti-angiogenic treatment in rat glioma. PLoS One 2010;5:e8727. [PubMed: 20090952]
35. Raatschen HJ, Simon GH, Fu Y, et al. Vascular permeability during antiangiogenesis treatment: MR imaging assay results as biomarker for subsequent tumor growth in rats. Radiology 2008;247:391–399. [PubMed: 18372448]
36. Dafni H, Kim SJ, Bankson JA, et al. Macromolecular dynamic contrast-enhanced (DCE)-MRI detects reduced vascular permeability in a prostate cancer bone metastasis model following anti-platelet-derived growth factor receptor (PDGFR) therapy, indicating a drop in vascular endothelial growth factor receptor (VEGFR) activation. Magn Reson Med 2008;60:822–833. [PubMed: 18816866]
37. Vogel-Claussen J, Gimi B, Artemov D, et al. Diffusion-weighted and macromolecular contrast enhanced MRI of tumor response to antivascular therapy with ZD6126. Cancer Biol Ther 2007;6:1469–1475. [PubMed: 17881899]
38. Bhujwalla ZM, Artemov D, Natarajan K, et al. Reduction of vascular and permeable regions in solid tumors detected by macromolecular contrast magnetic resonance imaging after treatment with antiangiogenic agent TNP-470. Clin Cancer Res 2003;9:355–362. [PubMed: 12538488]
39. Gilad AA, Israely T, Dafni H, et al. Functional and molecular mapping of uncoupling between vascular permeability and loss of vascular maturation in ovarian carcinoma xenografts: the role of stroma cells in tumor angiogenesis. Int J Cancer 2005;117:202–211. [PubMed: 15880497]
40. Bhujwalla ZM, Artemov D, Ballesteros P, et al. Combined vascular and extracellular pH imaging of solid tumors. NMR Biomed 2002;15:114–119. [PubMed: 11870907]
41. Penet MF, Pathak AP, Raman V, et al. Noninvasive multiparametric imaging of metastasis-permissive microenvironments in a human prostate cancer xenograft. Cancer Res 2009;69:8822–8829. [PubMed: 19861534]
42. Daldrup-Link HE, Brasch RC. Macromolecular contrast agents for MR mammography: current status. Eur Radiol 2003;13:354–365. [PubMed: 12599002]
43. Cyran CC, Fu Y, Raatschen HJ, et al. New macromolecular polymeric MRI contrast agents for application in the differentiation of cancer from benign soft tissues. J Magn Reson Imaging 2008;27:581–589. [PubMed: 18219614]

44. Preda A, Novikov V, Moglich M, et al. MRI monitoring of Avastin antiangiogenesis therapy using B22956/1, a new blood pool contrast agent, in an experimental model of human cancer. J Magn Reson Imaging 2004;20:865–873. [PubMed: 15503324]
45. Feng Y, Jeong EK, Mohs AM, et al. Characterization of tumor angiogenesis with dynamic contrast-enhanced MRI and biodegradable macromolecular contrast agents in mice. Magn Reson Med 2008;60:1347–1352. [PubMed: 19025902]
46. Senger DR, Brown LF, Claffey KP, et al. Vascular permeability factor, tumor angiogenesis and stroma generation. Invasion Metastasis 1994;14:385–394. [PubMed: 7544775]
47. Senger DR, Van de Water L, Brown LF, et al. Vascular permeability factor (VPF, VEGF) in tumor biology. Cancer Metastasis Rev 1993;12:303–324. [PubMed: 8281615]
48. Ferrara N. Role of vascular endothelial growth factor in regulation of physiological angiogenesis. Am J Physiol Cell Physiol 2001;280:C1358–C1366. [PubMed: 11350730]
49. Plaks V, Kalchenko V, Dekel N, et al. MRI analysis of angiogenesis during mouse embryo implantation. Magn Reson Med 2006;55:1013–1022. [PubMed: 16598729]
50. Plaks V, Birnberg T, Berkutzki T, et al. Uterine DCs are crucial for decidua formation during embryo implantation in mice. J Clin Invest 2008;118:3954–3965. [PubMed: 19033665]
51. Vandoorne K, Magland J, Plaks V, et al. Bone vascularization and trabecular bone formation are mediated by PKBalpha/Akt1 in a gene dosage dependent manner: In vivo and ex vivo MRI. Magn Reson Med. 2010 in press.
52. Ziv K, Nevo N, Dafni H, et al. Longitudinal MRI tracking of the angiogenic response to hind limb ischemic injury in the mouse. Magn Reson Med 2004;51:304–311. [PubMed: 14755656]
53. Pathak AP, Artemov D, Ward BD, et al. Characterizing extravascular fluid transport of macromolecules in the tumor interstitium by magnetic resonance imaging. Cancer Res 2005;65:1425–1432. [PubMed: 15735030]
54. Saban MR, Towner R, Smith N, et al. Lymphatic vessel density and function in experimental bladder cancer. 2007;7:219.
55. Dafni H, Cohen B, Ziv K, et al. The role of heparanase in lymph node metastatic dissemination: dynamic contrast-enhanced MRI of Eb lymphoma in mice. Neoplasia 2005;7:224–233. [PubMed: 15799822]
56. Israely T, Dafni H, Granot D, et al. Vascular remodeling and angiogenesis in ectopic ovarian transplants: a crucial role of pericytes and vascular smooth muscle cells in maintenance of ovarian grafts. Biol Reprod 2003;68:2055–2064. [PubMed: 12606340]
57. Israely T, Dafni H, Nevo N, et al. Angiogenesis in ectopic ovarian xenotransplantation: multiparameter characterization of the neovasculature by dynamic contrast-enhanced MRI. Magn Reson Med 2004;52:741–750. [PubMed: 15389965]
58. Ebert SN, Taylor DG, Nguyen HL, et al. Noninvasive tracking of cardiac embryonic stem cells in vivo using magnetic resonance imaging techniques. Stem Cells 2007;25:2936–2944. [PubMed: 17690182]
59. Zhou B, Shan H, Li D, et al. MR tracking of magnetically labeled mesenchymal stem cells in rats with liver fibrosis. Magn Reson Imaging. 2010
60. Madisen L, Zwingman TA, Sunkin SM, et al. A robust and high-throughput Cre reporting and characterization system for the whole mouse brain. Nat Neurosci 2010;13:133–140. [PubMed: 20023653]
61. Granot D, Addadi Y, Kalchenko V, et al. In vivo imaging of the systemic recruitment of fibroblasts to the angiogenic rim of ovarian carcinoma tumors. Cancer Res 2007;67:9180–9189. [PubMed: 17909023]
62. Granot D, Kunz-Schughart LA, Neeman M. Labeling fibroblasts with biotin-BSA-GdDTPA-FAM for tracking of tumor-associated stroma by fluorescence and MR imaging. Magn Reson Med 2005;54:789–797. [PubMed: 16149062]
63. Long CM, Bulte JW. In vivo tracking of cellular therapeutics using magnetic resonance imaging. Expert Opin Biol Ther 2009;9:293–306. [PubMed: 19216619]
64. Frank JA, Miller BR, Arbab AS, et al. Clinically applicable labeling of mammalian and stem cells by combining superparamagnetic iron oxides and transfection agents. Radiology 2003;228:480–487. [PubMed: 12819345]

65. Baligand C, Vauchez K, Fiszman M, et al. Discrepancies between the fate of myoblast xenograft in mouse leg muscle and NMR label persistency after loading with Gd-DTPA or SPIOs. Gene Ther 2009;16:734–745. [PubMed: 19282845]

66. Liu W, Frank JA. Detection and quantification of magnetically labeled cells by cellular MRI. Eur J Radiol 2009;70:258–264. [PubMed: 18995978]

67. Wang Z, Tiruppathi C, Minshall RD, et al. Size and dynamics of caveolae studied using nanoparticles in living endothelial cells. ACS Nano 2009;3:4110–4116. [PubMed: 19919048]

68. Vogel SM, Minshall RD, Pilipovic M, et al. Albumin uptake and transcytosis in endothelial cells in vivo induced by albumin-binding protein. Am J Physiol Lung Cell Mol Physiol 2001;281:L1512–L1522. [PubMed: 11704548]

69. Phung TL, Ziv K, Dabydeen D, et al. Pathological angiogenesis is induced by sustained Akt signaling and inhibited by rapamycin. Cancer Cell 2006;10:159–170. [PubMed: 16904613]

70. Gilead A, Meir G, Neeman M. The role of angiogenesis, vascular maturation, regression and stroma infiltration in dormancy and growth of implanted MLS ovarian carcinoma spheroids. Int J Cancer 2004;108:524–531. [PubMed: 14696116]

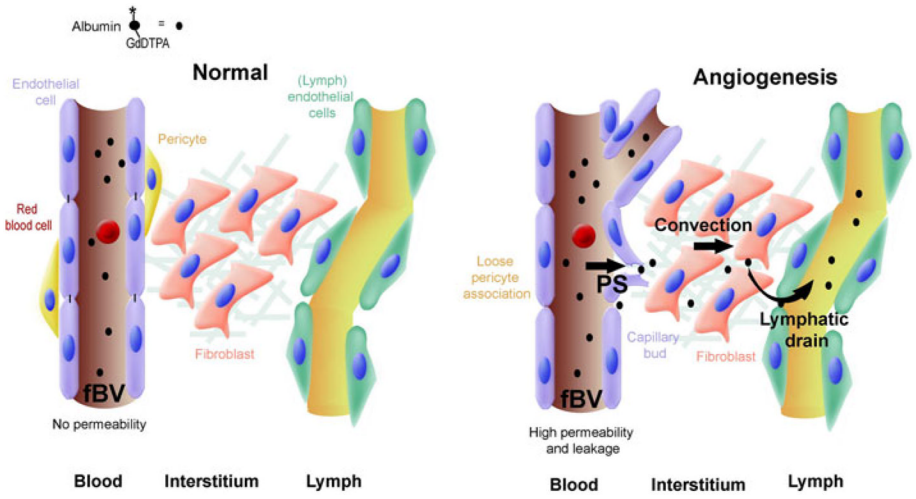

Fig. 1.

Measurement of vascular permeability, interstitial convection and lymphatic drain using tagged albumin. (*Left*) In normal tissue with mature blood vessels, after intravenous injection, albumin-GdDTPA does not extravasate, and its concentration inside the blood vessels slowly decreases ($t_{1/2}$ = 4 h). (*Right*) During angiogenesis blood vessels are hyperpermeable. Initially, the contrast agent is only in the vessels, yielding an estimation of the microvascular density (fBV). The rate (or slope) of interstitial accumulation of the contrast agent provides the permeability surface area product (or permeability; PS). Elevated interstitial pressure, for example in the center of a tumor, can drive interstitial convection (convection). Eventually after a longer period (>60 min) the extravasated albumin-GdDTPA is drained from the interstitium into the lymphatics

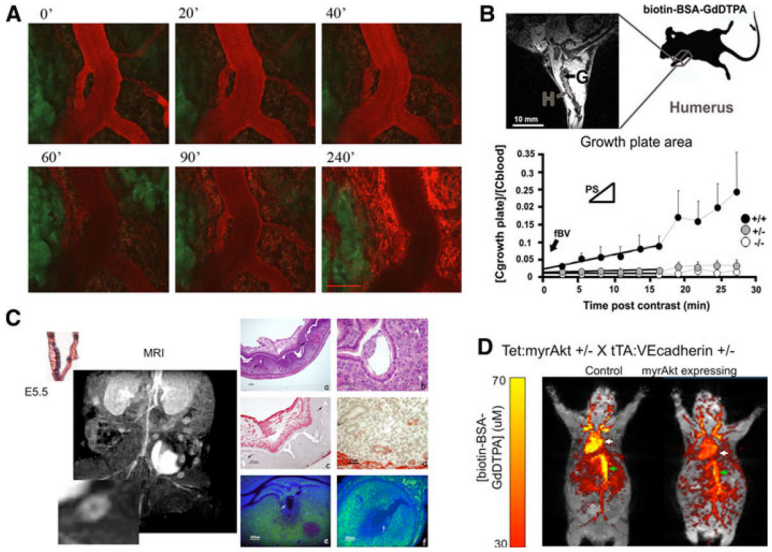

Fig. 2.

MRI and fluorescence imaging of vascular permeability. **a** Confocal intravital microscopy of angiogenic vasculature of an MLS ovarian tumor implanted in a dorsal skin flap chamber. BSA-Rhodamine (ROX) was administered intravenously and followed for 4 h. Time points 0–90 min were acquired without moving the animal. Point 120 & 240 min were acquired after the animal was awake and re-anesthesized for continued imaging (*bar*, 100 micron). **b** Analysis of blood vessel permeability in the growing bone, showing difference between the permeable vessels in wild-type (+/+) mice relative to the non permeable vessels in PKBalpha/Akt1 heterozygous (±) or knockout (−/−) mice [51]. **c** Vascular permeability enhanced in sites of fetal implantation. (*Left*) MRI after administration of biotin-BSA-GdDTPA (*inset*; magnification of a single implantation site). (*Right*) histological analysis of implantation sites showing H&E staining (**a**, **b**), vascular alphaSMA staining of mature vessels (**c**, **d**) and histological analysis of the contrast media (**e**, **f**) [49]. **d** MRI analysis of systemic vascular expansion and elevated permeability induced by endothelial expression of activated PKBalpha/Akt1. Color scale, concentration of biotin-BSA-GdDTPA [69]

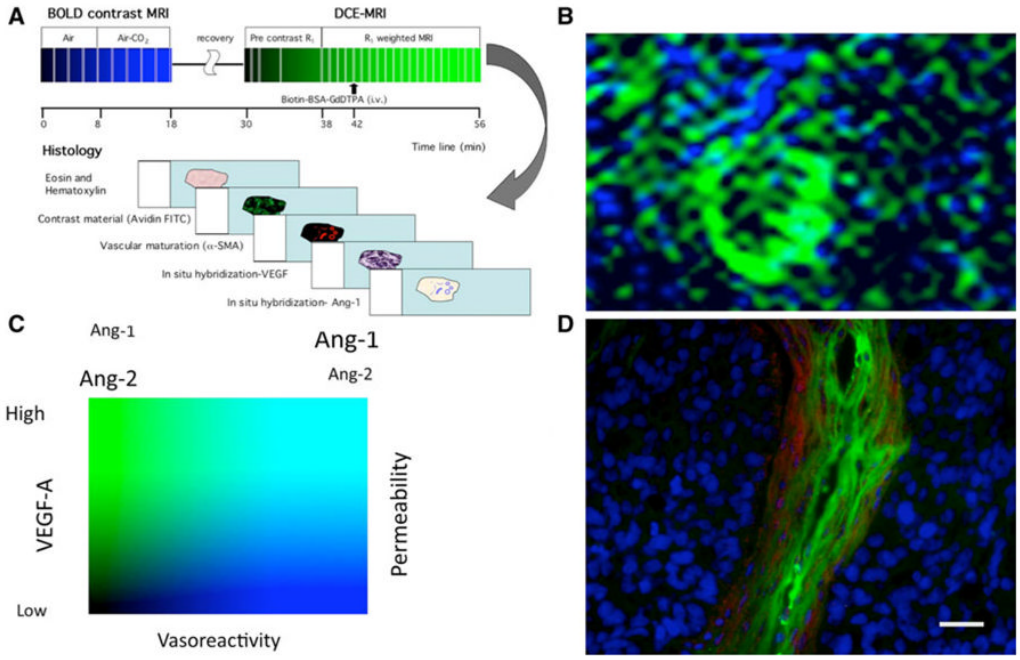

Fig. 3.

Multiparametric mapping of vascular permeability and vascular maturation. **a** Consecutive BOLD contrast response to hypercapnia and DCE-MRI followed by histological analysis can be used for mapping vascular maturation and permeability. **b** Map of vasoreactivity to hypercapnia (in *blue*) and vascular permeability to biotin-BSA-GdDTPA (in *green*) of an ovarian carcinoma xenograft, showing the high vasoreactivity and low permeability of the normal tissue and the high permeability and low vasoreactivity characteristic of the tumor vessels. **c** Vasoreactivity and vascular permeability as functional biomarkers for the activity of angiogenic growth factors such as the relative fraction of angiopoietins 1 and 2 that control vascular maturation and VEGF as a regulator of vascular permeability. **d** Fluorescence imaging of vascular permeability (*green*; avidin-FITC staining of biotin-BSA-GdDTPA) and maturation (*red*; alpha-SMA staining of pericytes, vascular smooth muscle cells and myofibroblasts) in histological section of an ovarian carcinoma tumor [39,70]

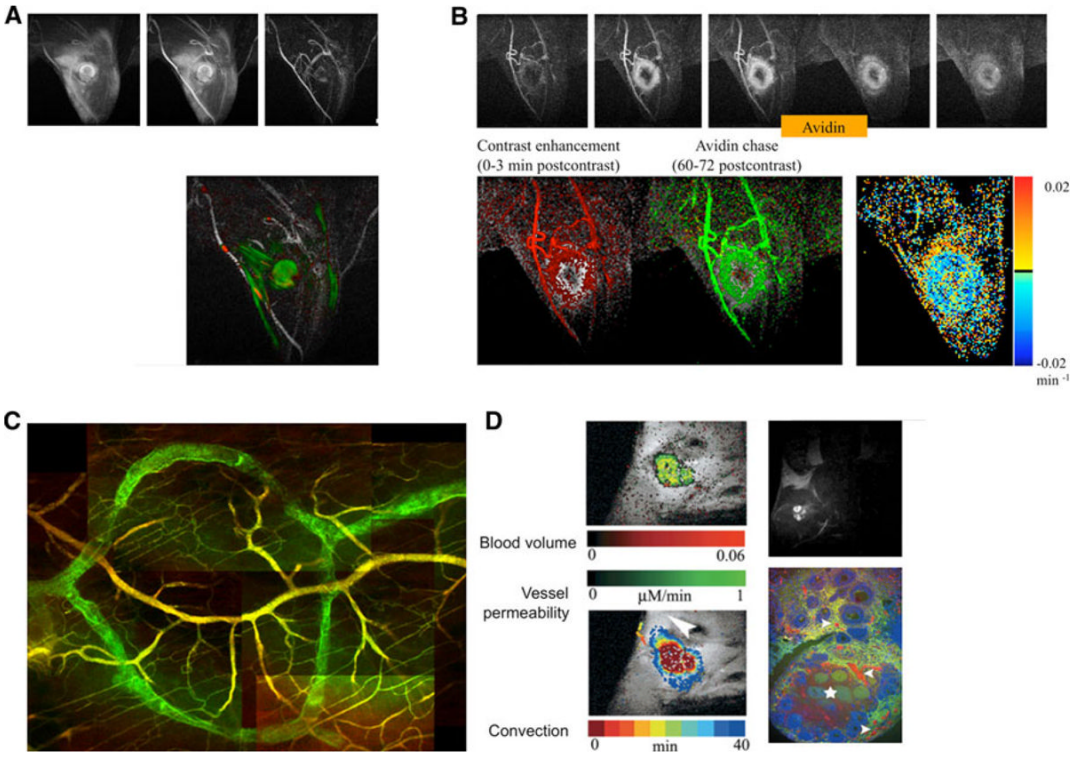

Fig. 4.

Imaging permeability, convection and lymphatic drain using biotin-BSA-GdDTPA (FAM/ROX). **a** Delayed enhancement observed in a mouse in which biotin-BSA-GdDTPA was administered intravenously and allowed to circulate for 6 h (*green*) and 3 min (*red*). Contrast material extravasated from the VEGF over expressing tumor in the limb of the mouse and drained towards the popliteal lymph node. **b** In vivo avidin chase analysis of lymphatic clearance. Administration of avidin results in immediate clearance of the intravascular contrast media. *Lower row: left*, initial enhancement angiogram (*red*); center, avidin induced clearance (*green*); *right*, life time for interstitial albumin clearance [16,30]. **c** Fluorescence imaging of lymphatic uptake of extravasated albumin (lymphatic vessels, biotin-BSA-GdDTPA-FAM, green; blood vessels, BSA-ROX, *red*). **d** Angiogenesis of ovarian grafts, showing high convection and lymphatic drain of extravasated biotin-BSA-GdDTPA [56,57]

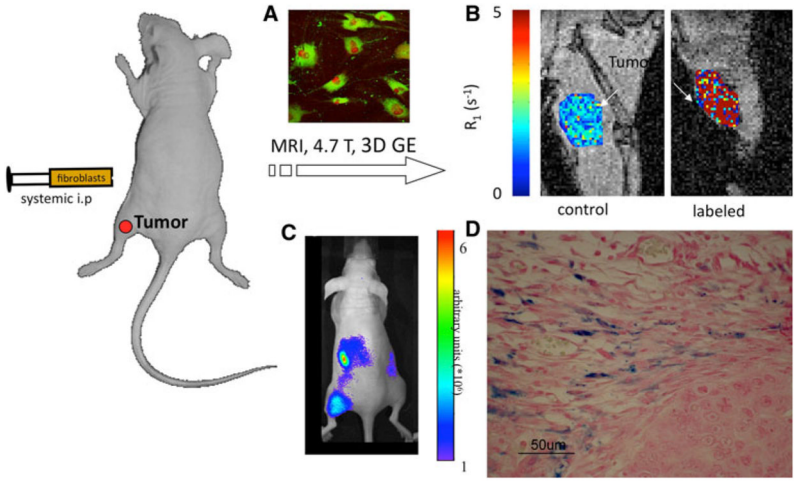

Fig. 5.

Recruitment of fibroblasts detected using tagged albumin. **a** Fluorescence microscopy of fibroblasts incubated with biotin-BSA-GdDTPA (*green*). **b** MRI analysis showing elevated R1 in subcutaneous ovarian carcinoma tumors when labeled fibroblasts were administered intraperitonealy and recruited to the tumor. **c** NIR imaging showing recruitment of DiR labeled fibroblasts. **d** Histological Prussian Blue staining showing recruitment of iron-oxide labeled fibroblasts to ovarian carcinoma tumors [61,62]